Recurrent Supersynoptic Evolution of the Great Plains Low-Level Jet

SCOTT J. WEAVER

NOAA/Climate Prediction Center, Camp Springs, Maryland

SUMANT NIGAM

Department of Atmospheric and Oceanic Science, and Earth System Science Interdisciplinary Center, University of Maryland, College Park, College Park, Maryland

ABSTRACT

The evolution of supersynoptic (i.e., pentad) Great Plains low-level jet (GPLLJ) variability, its precipitation impacts, and large-scale circulation context are analyzed in the North American Regional Reanalysis (NARR)—a high-resolution precipitation-assimilating dataset—and the NCEP–NCAR reanalysis. The analysis strategy leans on the extended EOF technique, which targets both spatial and temporal recurrence of a variability episode.

Pentad GPLLJ variability structures are found to be spatially similar to those in the monthly analysis. The temporal evolution of the supersynoptic GPLLJ-induced precipitation anomalies reveal interesting lead and lag relationships highlighted by GPLLJ variability-leading precipitation anomalies. Interestingly, similar temporal phasing of the GPLLJ and precipitation anomalies were operative during the 1993 (1988) floods (drought) over the Great Plains, indicating the importance of these submonthly GPLLJ variability modes in the instigation of extreme hydroclimatic episodes. The northward-shifted (dry) GPLLJ variability mode is linked to large-scale circulation variations emanating from remote regions that are modified by interaction with the Rocky Mountains, suggesting that the supersynoptic GPLLJ fluctuations may have their origin in orographic modulation of baroclinic development.

1. Introduction

The recent calls for U.S. climate prediction strategies to bridge the gap between 2-week deterministic weather forecasts and seasonal climate predictions, as well as the growing societal need for regional climate forecast information, warrant an investigation of supersynoptic mechanisms of hydroclimate variability, especially during the agriculturally important warm season. Nowhere is this more important than over the Great Plains, for this region is prone to significant warm season climate fluctuations, highlighted most recently by extreme hydroclimate anomalies in 1988, 1993, and 2008 that caused massive socioeconomic and ecological consequences.

Of particular importance to warm season central U.S. hydroclimate variability is the Great Plains low-level jet (GPLLJ). Precipitation variations are extremely sensitive to this recurring climatic feature of the circulation. GPLLJ variability refers to fluctuations in strength, placement, and timing of the GPLLJ that exert a profound influence on the regional hydroclimate of the central United States (Cook et al. 2008). Efforts to more fully understand the origins of GPLLJ fluctuations have uncovered linkages to large-scale atmospheric circulation variability (Byerle and Paegle 2003; Ting and Wang 2006; Weaver and Nigam 2008; Weaver et al. 2009a), thermal and orographic influences (Holton 1967; Ting and Wang 2006; Wexler 1961), and recurring modes of global-scale SST variability (Weaver et al. 2009b).

Most recently, Weaver and Nigam (2008, hereinafter WN) applied EOF analysis to the lower-tropospheric wind field using 24 years (1979–2002) of monthly averaged data from the North American Regional Reanalysis (NARR). The first three modes of GPLLJ variability were shown to be quite influential in focusing Great Plains precipitation anomalies, with modes 1 and 3 important for the 1993 flood and mode 2 for the 1988 drought. The

Corresponding author address: Dr. Scott J. Weaver, Climate Prediction Center, NOAA/NWS/NCEP, 5200 Auth Road, Rm. 605, Camp Springs, MD 20746.
E-mail: scott.weaver@noaa.gov

position and spatial structure of the GPLLJ were found to be as important as its magnitude in generating the precipitation anomalies. Recently, Weaver et al. (2009a, hereinafter WRBN) showed that the supersynoptic fluctuations of the GPLLJ were instrumental in generating the extreme precipitation anomalies during 1988 (drought) and 1993 (flood), and that these fluctuations temporally led the precipitation and moisture flux convergence development by as much as two pentads during those events.

The purpose of this note is to extend the characterization of GPLLJ variability to submonthly time scales. The characterization will lay a foundation for future investigations of GPLLJ predictability on intraseasonal time scales and provide a basis for interpreting the origin of the monthly modes of GPLLJ variability (WN). Additionally, the proposed analysis will reveal if the submonthly evolution of the GPLLJ during extreme hydroclimate episodes (described in WRBN at pentad resolution) is a manifestation of the recurring modes of supersynoptic GPLLJ variability identified in this note. The focus is on the evolution of GPLLJ variability, the related precipitation signal, and the large-scale circulation in which the GPLLJ variation is embedded.

The dataset of choice is the high-resolution precipitation and radiance-assimilating NARR. NARR's representation of North American hydroclimate is deemed superior to that in widely used global reanalyses [e.g., National Centers for Environmental Prediction (NCEP)–National Center for Atmospheric Research (NCAR) and the 40-yr European Centre for Medium-Range Weather Forecasts (ECMWF) Re-Analysis (ERA-40)] on account of its successful assimilation of precipitation (Mesinger et al. 2006), notwithstanding the existence of regional water-balance errors in its atmospheric and terrestrial branches (WRBN). The analysis leans on the extended EOF technique (Weare and Nasstrom 1982) in extraction of the preferred modes of spatial and temporal variability of the GPLLJ, as opposed to traditional EOF analysis, which identifies only the spatially recurrent patterns. The former is more insightful as it isolates the preferred spatially evolving developments (from the nascent to mature phase)—potentially, the entire span of recurrent episodes.

Questions we wish to examine include the following:

(i) What is the structure and evolution of the preferred modes of GPLLJ variability on supersynoptic time scales?

(ii) How does regional precipitation evolve in response to supersynoptic GPLLJ variability?

(iii) What is the role of the large-scale and/or remotely generated circulations in the evolution of supersynoptic GPLLJ variability?

Section 2 details the NARR dataset and analysis strategy. Section 3 highlights the spatiotemporal patterns of GPLLJ variability and the evolution of hydroclimate impacts. Section 4 documents the large-scale circulation related to jet variability, while concluding remarks follow in section 5.

2. Datasets and methodology

The NARR is a 27-yr (1979–2005), consistent, high-resolution dataset that covers the North American domain (Mesinger et al. 2006). The original NARR has a 3-h analysis cycle and 32-km horizontal resolution. The data used here have been regridded to $0.5° \times 0.5°$. There are 13 vertical levels (29 total) below 700 hPa, which are adequate for resolving the prominent regional circulation feature—the shallow GPLLJ. NARR assimilates direct observations of precipitation over land and adjoining oceanic regions using the upgraded regional eta model and related data assimilation system. The precipitation assimilation is shown to be successful under the influence of a two-way interaction with the Noah land surface model (Ek et al. 2003; Mesinger et al. 2006). Given NARR's regional domain, the large-scale circulation fields are obtained, as needed, from the NCEP–NCAR reanalysis (Kalnay et al. 1996).

Pentad averages (5-day means) are analyzed in this study, unless otherwise noted. NARR pentads were created by averaging the 3-hourly data, while the NCEP–NCAR reanalysis pentad data were produced from daily means. In leap years, the pentad beginning on 25 February is a 6-day average so as to keep the number of pentads (73) per year consistent throughout the 27-yr NARR record (1979–2005). All anomalies are with respect to their pentad climatology unless otherwise stated.

The extended empirical orthogonal function (EEOF) analysis is a powerful technique for extracting spatiotemporal recurrence (Weare and Nasstrom 1982)—not just spatial or temporal, as in traditional EOFs. The additional focus on temporal recurrence yields spatially *and* temporally coherent patterns, generating insights into antecedent/subsequent phases, and thus modal evolution and mechanisms. The technique's emphasis on evolution obviates the need for data prefiltering because similar-looking, overlapping patterns that evolve differently can now be easily separated. Also, the pre- and postmature phase patterns identified from EEOF analysis need not bear any resemblance to the mature phase structure—the case (and limitation) in lead/lag regression analysis.

The technique is a straightforward extension of EOF analysis, except for the new anomaly definition: anomalies at time $t = t_o$ are no longer field snapshots at that time [i.e.,

$\psi(x, y, t_o)$], but a snapshot sequence centered at $t = t_o$. Using 3-member overlapping pentads, the anomaly at $t = t_o$ is a sequence of 3 spatial patterns that are staggered in time [$\psi(x, y, t_o - \Delta t)$, $\psi(x, y, t_o)$, $\psi(x, y, t_o + \Delta t)$]. The interval, Δt, is chosen so that the temporal sequence covers a significant portion of the variability episode. Note that there is no imposition of any periodicity here, unlike some other methods that target evolution.

EOF and EEOF analysis are performed on the May-to-July (MJJ) pentad (5 day) averaged 900-hPa meridional winds, using 3 pentad sequences. Targeting late spring/early summer maintains seasonal consistency with the WN and WRBN analyses. The covariance matrix was used in the EEOF calculation. Lead/lag regressions of the derived principal components on hydroclimate variables help characterize the GPLLJ-linked hydroclimate episodes; temporal phasing and magnitude included. In this analysis, the MJJ period is defined as 16 pentads, beginning with the first full pentad in May. Pentad averaging eliminates diurnal and much of the synoptic variability, while retaining lower-frequency (submonthly) climatic fluctuations. The potential sensitivity to the evolving seasonal cycle is assessed by performing the analysis, separately, on the first and second halves of the MJJ period; the sensitivity is insignificant.

3. Recurrent supersynoptic variability of the GPLLJ

a. Time scales

The autocorrelation structure of the extracted principal components (PCs) is first analyzed to discern the time scale of the related spatiotemporal variability patterns. Given our interest in supersynoptic variability, the structure is shown only for the long-lived patterns (Fig. 1); the autocorrelation of the first principal component derived from traditional EOF analysis is also shown for reference. The EOF1-PC autocorrelation is quite small at even ± 1 pentad, indicating that the EOF1 pentad resolution portrayal remains dominated by high-frequency (synoptic scale) variability. Autocorrelation of PCs associated with EEOFs 2, 3, and 5 falls off even more rapidly (not shown). The PCs exhibiting the highest autocorrelation at ± 1 pentad (and beyond) are EEOFs 1 and 4, which explain 13.4% and 8.8% of the variance, respectively. Crossings of the e^{-1} threshold suggest ~4-pentad duration for these two variability modes. As such, these two modes exhibit the best prospects for advancing submonthly predictability of the GPLLJ variations and their hydroclimate impacts. Interestingly, the loading vectors of these modes are quite similar to those of the leading monthly patterns (cf. Fig. 10 in WN).
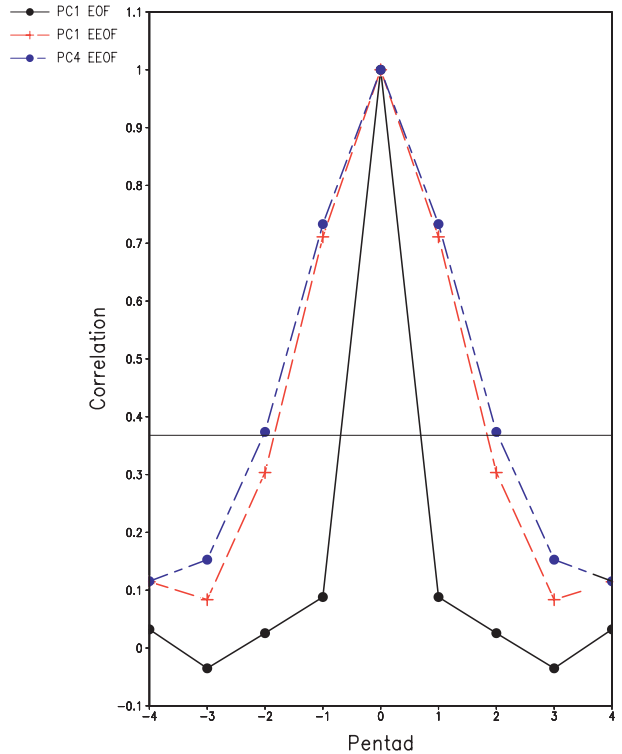

FIG. 1. Autocorrelation of the pentad resolution EOF1-PC (black) and PCs 1 and 4 (colors) generated from EEOF analysis. The horizontal line denotes the e^{-1} demarcation.

b. Spatiotemporal evolution and precipitation impact

A key advantage of extended-EOF analysis over the traditional one is its ability to capture recurrent, coherent evolution with spatially evolving patterns. The two analyses are compared in Fig. 2 in context of the leading variability mode; EOF1 in the left and EEOF1 in the right column. The antecedent and subsequent pattern in the EOF case is obtained from lag/lead regressions of the principal component, as is the precipitation impact in both cases. Both methods, evidently, yield similar mature phase patterns (leading to meridional expansion of the jet in the displayed phase)[1] and related hydroclimate impacts, but the EOF method is unable to portray evolution, including episode duration. A robust characterization of the nascent phase, in particular, would be helpful in the investigation of submonthly predictability. The precursor ($t = -1$ pentad) signal (as diagnosed in the EEOF analysis) is quite similar to the mature pattern, as expected from the relatively long life (~4 pentads) of this variability mode (cf. Fig. 1). The nascent phase ($t = -2$ pentad) jet

---

[1] The choice of the EOF display phase is, in essence, arbitrary. An opposite value of the PC will result in a sign reversal of the loading pattern.
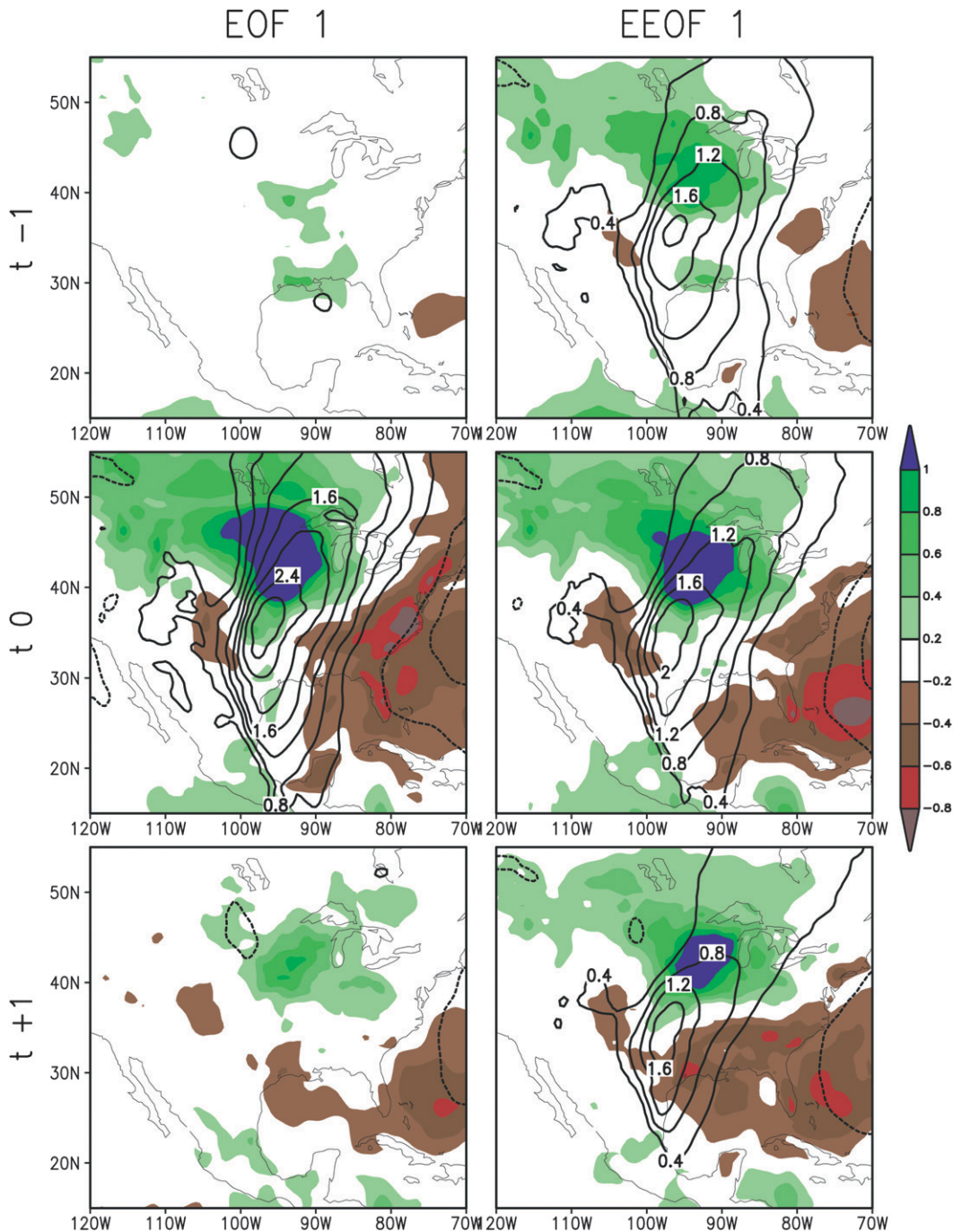
FIG. 2. Pentad evolution of the first mode of GPLLJ variability (contoured) and regressed precipitation anomalies (shaded) from $t = -1$ to $t + 1$. (left) Traditional EOF analysis; (right) the EEOF analysis. Precipitation is shaded at 0.2-mm day^{-1} intervals while the GPLLJ is contoured at 0.4 m s^{-1}.

anomaly has a different structure but weak amplitudes ($\sim$0.3 m s^{-1}), and is, as such, not shown. The jet remains strong in the core region in the postmature phase ($t = +1$ pentad) which is marked by significant zonal and meridional contraction vis-à-vis prior jet structure.

The precipitation signal exhibits interesting development as well: the signal is strongest ($\sim$1 mm day^{-1}) when the jet anomaly is at its peak, but a less-than-1 pentad lead/lag is possible given the analysis resolution. Inspection of the $t + 1$ pentad distributions, in fact, suggests that

precipitation lags jet development. The precipitation signal is large relative to the jet anomaly in these maps; the $t - 1$ maps provide context for this assessment. The lead of the GPLLJ perturbation vis-à-vis the precipitation signal was recently noted in WRBN in context of the 1993 Great Plains flood.

The low-level jet and precipitation evolution associated with the other slowly varying EEOF is shown in Fig. 3. The jet anomaly of the fourth EEOF is quite similar to monthly EOF2 in WN (cf. their Fig. 10), and leads to a northward-displaced GPLLJ over a 3-pentad period, accompanied by significant precipitation reduction over the eastern half of the continent, with a central–southern Great Plains focus. The precipitation impact is not surprising given the jet's weakened connection to the Gulf of Mexico in the displayed phase—the primary moisture source for summertime precipitation variability. Note the weak positive precipitation anomaly in the jet exit region at $t = +1$ pentad, arising mainly from the persistence of the kinematic convergence ($-\partial v/\partial y$), as this anomaly is not evident at $t = 0$.

It would be interesting to assess the evolution of PCs 1 and 4 during the drought of 1988 and flood of 1993 over the Great Plains. Figure 4 shows the pentad evolution of PC1 (solid blue) and PC4 (solid red) from the EEOF analysis, and PC1 from the EOF analysis (blue dashed) for 1988 (top panel) and 1993 (bottom panel). It is worth noting that the 1993 flood was mostly due to EEOF1 (with a weak contribution from the reverse phase of EEOF4), unlike in 1988, when EEOF4 had some support from the opposite phase of EEOF1.

Furthermore, the EEOF mode 1 (mode 4) time series do compare nicely with the total anomaly evolution during 1993 (1988) (cf. WRBN, their Fig. 3) save for the early-June jet episode in 1993, which interestingly appears in the 1-pentad spike of EOF1 PC (Fig. 4). The EEOF mode 1 representation during this time shows a slower evolution highlighted by increasing amplitude. However, a closer inspection of the total precipitation anomaly during this 1-pentad spike shows only a weak positive anomaly in the presence of a quick- and strong-amplitude GPLLJ event (as evidenced in the 1-pentad EOF spike), further suggesting that a lower-frequency evolution (as shown in the EEOF analysis) is more apt to produce a long-lived and significant precipitation anomaly, as seen in early July 1993.

c. Moisture flux convergence

Recent studies have shown that remote water sources contribute substantially to Great Plains hydroclimate variability in summer through moisture transports enabled by regional circulation features (Ruiz-Barradas and Nigam
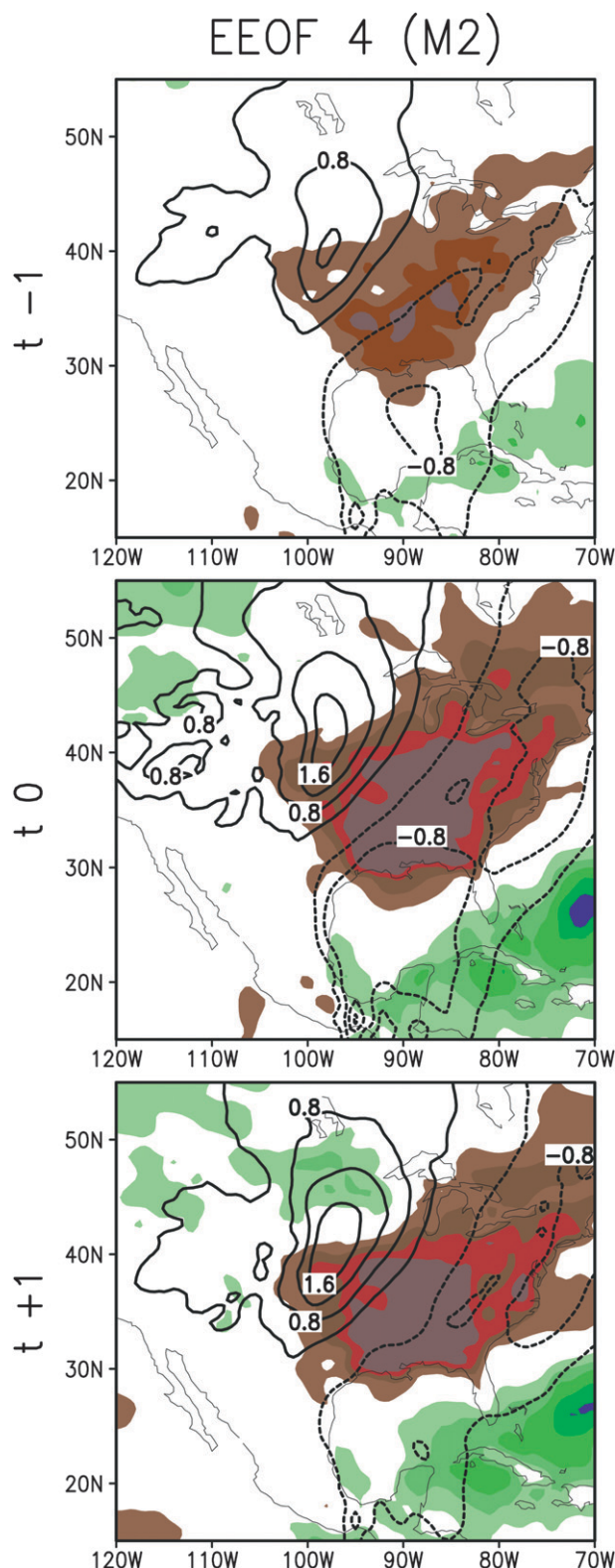

FIG. 3. Pentad evolution of the fourth EEOF mode of GPLLJ variability (contoured) and regressed precipitation anomalies (shaded) from $t = -1$ to $t = +1$. Precipitation is shaded at 0.2 mm day^{-1} intervals while the GPLLJ is contoured at 0.4 m s^{-1}.
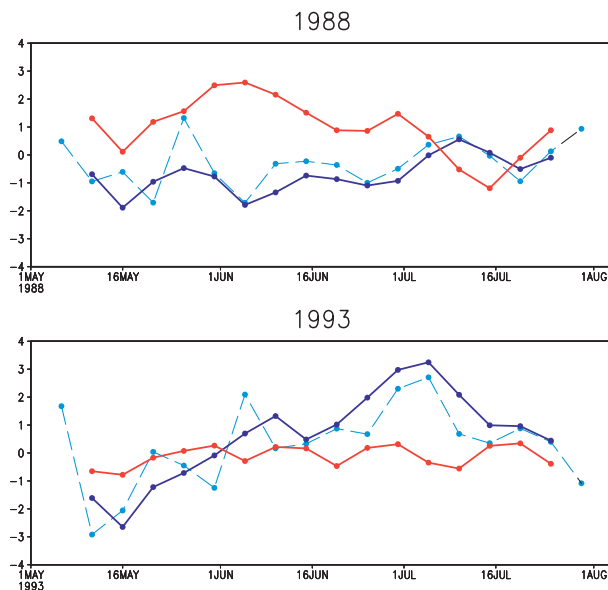
FIG. 4. Comparison of pentad GPLLJ PC time series during the (top) 1988 drought and (bottom) 1993 flood from the EOF mode 1 (light blue dashed), EEOF mode 1 (solid blue), and EEOF mode 4 (solid red).

2005; WN and references therein). Figure 5 shows the moisture flux convergence in the mature phase pentad ($t = 0$), obtained from PC regressions on the column-integrated stationary and transient moisture flux convergence $-\int_{300\text{hPa}}^{P_{\text{surface}}} \nabla \cdot (q\mathbf{V})g^{-1}\,dp$, where q is 3-hourly specific humidity, $\mathbf{V}$ the 3-hourly horizontal wind, and g the gravity. The column-integrated convergence is contoured just as precipitation to facilitate visual assessment of the regional atmospheric water balance. Moisture flux convergence evidently accounts for both the pattern and amplitude of the precipitation signal for both modes rather well, attesting to the importance of GPLLJ fluctuations in generating intense, pentad-time-scale hydroclimate variability over the eastern half of the continent.

4. Large-scale circulation context of the supersynoptic GPLLJ fluctuations

Given the key role of GPLLJ fluctuations in generation of summer hydroclimate variability over the central and eastern United States, and the implication of remotely generated (from adjoining ocean basins) circulation anomalies in drought generation (e.g., Ruiz-Barradas et al. 2010), it is of some interest to examine the large-scale circulation anomalies in which the leading, supersynoptic GPLLJ fluctuations are embedded. We focus on the mode that moves the GPLLJ northward (Fig. 3), as this mode—connected to precipitation reduction over the eastern continent—was notably strong during the 1988 summer drought (WN).
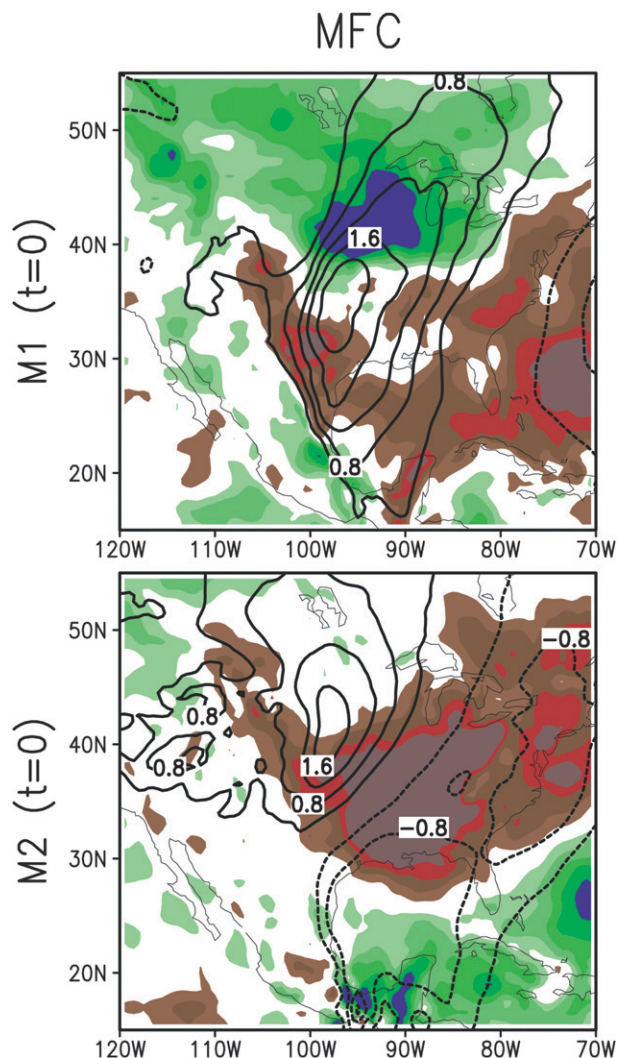

FIG. 5. The mature phase (i.e., at time zero) of the (top) first and (bottom) fourth EEOF modes of GPLLJ (contoured) and column-integrated moisture flux convergence (shaded). Moisture flux convergence is shaded at 0.2 mm day^{-1} intervals while the GPLLJ is contoured at 0.4 m s^{-1}.

The propagated responses to wave forcing regions, including tropical–extratropical links, are typically manifest in the upper troposphere. A large-scale circulation context is provided by the 200-hPa geopotential height (Fig. 6) derived from lead/lag regressions of the PC time series from EEOF4. A coherent signal extending from the midlatitude North Pacific to the eastern seaboard (and beyond) is present, at least, from the $t = -1$ pentad onward. Although the trough and ridge placements line up with the circumglobal teleconnection structure over the Pacific–North American sector [e.g., Figs. 5a,c in Ding and Wang (2005)], corresponding height correlations reveal only the North American sector signal (West Coast trough, ridge over the central–northern plains, and the
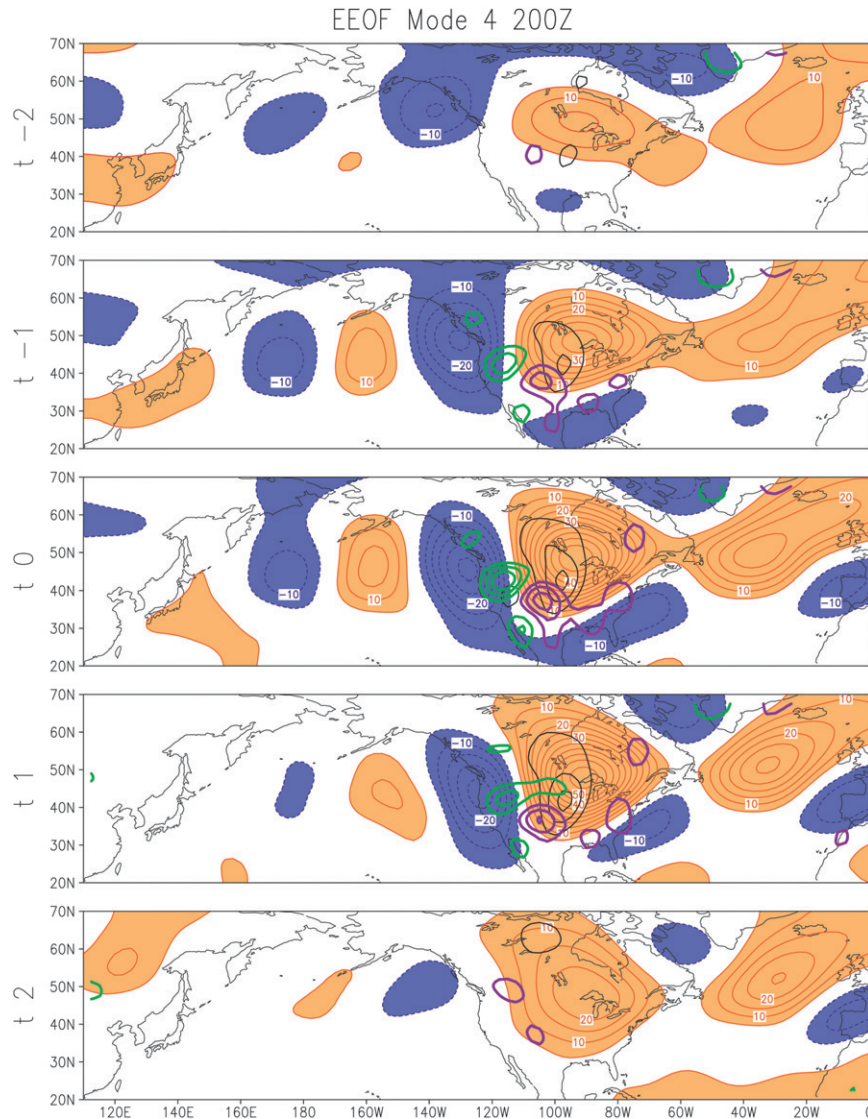
EEOF Mode 4 200Z

FIG. 6. Pentad evolution of the GPLLJ (black contours), 850-hPa divergence (green and purple contours), and 200-hPa height (shaded) for EEOF mode 4 from pentad -2 to pentad $+2$. Negative (positive) 200-hPa anomalies are shaded in blue (orange) and contoured at 5-m intervals, while negative (positive) 850-hPa divergence anomalies are contoured at 3×10^{-6} s^{-1} intervals in green (purple) beginning at $\pm 2 \times 10^{-6}$ s^{-1}.

Gulf Coast trough) to be significant, and that too from the $t - 1$ to $t + 2$ pentad. The height anomalies are equivalent barotropic but with a slight westward tilt with height (although not as pronounced as in synoptic baroclinic development, not shown). The 850-hPa anomalies (not shown), with bearing on the GPLLJ, are thus somewhat eastward positioned, with the western flank of the ridge aligned with the southerly jet perturbation.

The development dynamics are difficult to discern observationally, especially because pentad averages rather than pentad interval snapshots are displayed, which precludes careful estimation of the field tendencies. The flow

structure, however, leaves scope for significant orographic interaction, given the westerlies and southerlies impinging on the Rockies as part of the anomalous upstream cyclonic circulation, and easterlies as part of the continental anticyclone. The superposed 850-hPa divergence contains features arising from both quasigeostrophic dynamics (e.g., ascent, or convergence in the region between cyclone and anticyclone, i.e., in southerly region) and orographic effects (divergence in downslope and convergence in upslope regions).

The large-scale circulation analysis suggests that development of supersynoptic fluctuations of the GPLLJ

may have its origin in orographic modulation of baroclinic development.

5. Discussion

Supersynoptic evolution of GPLLJ variability and its related large-scale circulation and precipitation impacts are investigated in this note to ascertain the temporal phasing of submonthly hydroclimate anomalies over the central United States during the warm season. The analysis is notable for using the extended EOF analysis technique in an attempt to connect traditional analyses of monthly GPLLJ variability with the inherent supersynoptic underpinnings.

It is found that pentad GPLLJ spatial variability structures are similar to those derived from monthly analysis. The temporal evolution of the GPLLJ-related precipitation anomalies reveal interesting lead and lag relationships highlighted by GPLLJ variability-leading precipitation. The precipitation anomalies are shown to be primarily related to column-integrated moisture flux convergence, as this quantity can account for the entirety of the precipitation anomaly placement and amplitude. Interestingly, similar temporal phasing of the GPLLJ, precipitation, and moisture flux convergence anomalies was operative during the 1993 (1988) floods (drought) over the Great Plains (WN; WRBN), suggesting the importance of these submonthly GPLLJ variability modes in the instigation of extreme hydroclimatic episodes.

The connection to the large-scale circulation during the dry northward-displaced GPLLJ variability mode reveals a propagated response potentially instigated by tropical forcing, as also noted in WN. While the development dynamics is difficult to discern observationally, orographic modulation of the large-scale circulation appears important in the supersynoptic development of this GPLLJ variability mode. Elucidating the forcing mechanisms of warm season large-scale circulation anomalies and, by extension, supersynoptic GPLLJ variability modes may lead to enhanced Great Plains hydroclimate predictions and is the subject of ongoing research.

REFERENCES

Byerle, L. A., and J. Paegle, 2003: Modulation of the Great Plains low-level jet and moisture transports by orography and large-scale circulations. *J. Geophys. Res.,* **108,** 8611, doi:10.1029/2002JD003005.

Cook, K. H., E. K. Vizy, Z. S. Launer, and C. M. Patricola, 2008: Springtime intensification of the Great Plains low-level jet and Midwest precipitation in GCM simulations of the twenty-first century. *J. Climate,* **21,** 6321–6340.

Ding, Q., and B. Wang, 2005: Circumglobal teleconnection in the Northern Hemisphere summer. *J. Climate,* **18,** 3483–3505.

Ek, M. B., K. E. Mitchell, Y. Lin, E. Rogers, P. Grunmann, V. Koren, G. Gayno, and J. D. Tarpley, 2003: Implementation of Noah land surface model advances in the National Centers for Environmental Prediction operational mesoscale Eta model. *J. Geophys. Res.,* **108,** 8851, doi:10.1029/2002JD003296.

Holton, J. R., 1967: The diurnal boundary layer wind oscillation above sloping terrain. *Tellus,* **19,** 199–205.

Kalnay, E., and Coauthors, 1996: The NCEP/NCAR 40-Year Reanalysis Project. *Bull. Amer. Meteor. Soc.,* **77,** 437–471.

Mesinger, F., and Coauthors, 2006: North American Regional Reanalysis. *Bull. Amer. Meteor. Soc.,* **87,** 343–360.

Ruiz-Barradas, A., and S. Nigam, 2005: Warm season rainfall variability over the U.S. Great Plains in observations, NCEP and ERA-40 reanalyses, and NCAR and NASA atmospheric model simulations. *J. Climate,* **18,** 1808–1830.

——, and ——, 2010: Great Plains precipitation and its SST links in twentieth-century climate simulations, and twenty-first- and twenty-second-century climate projections. *J. Climate,* **23,** 6409–6429.

Ting, M., and H. Wang, 2006: The role of the North American topography on the maintenance of the Great Plains summer low-level jet. *J. Atmos. Sci.,* **63,** 1056–1068.

Weare, B. C., and J. S. Nasstrom, 1982: Examples of extended empirical orthogonal function analyses. *Mon. Wea. Rev.,* **110,** 481–485.

Weaver, S. J., and S. Nigam, 2008: Variability of the Great Plains low-level jet: Large-scale circulation context and hydroclimate impacts. *J. Climate,* **21,** 1532–1551.

——, A. Ruiz-Barradas, and S. Nigam, 2009a: Pentad evolution of the 1988 drought and 1993 flood over the Great Plains: An NARR perspective on the atmospheric and terrestrial water balance. *J. Climate,* **22,** 5366–5384.

——, S. Schubert, and H. Wang, 2009b: Warm season variations in the low-level circulation and precipitation over the central United States in observations, AMIP simulations, and idealized SST experiments. *J. Climate,* **22,** 5401–5420.

Wexler, H., 1961: A boundary layer interpretation of the low-level jet. *Tellus,* **13,** 368–378.